Mathematical Modeling and Algorithm Application
ISSN: 3006-0842 | Vol. 6, No. 3, 2025

A Study on Calculating Epitaxial Layer Thickness Based on a Multi-Parameter Collaborative Optimization Model

Huiming Chen

School of Advanced Manufacturing, Guangdong University of Technology, Guangzhou 510006, China

Abstract: Semiconductor materials have progressively become core components in chip manufacturing owing to their unique physical and chemical properties. Taking silicon carbide as an example, this paper establishes a computational model for parameters such as refractive index and epitaxial layer thickness during beam reflection. This model is based on the principles of reflection and transmission at the epitaxial layer-substrate interface, utilising beam reflection principles alongside the Drude model and Fresnel equations. Under specified conditions, this study performed global fitting on the dataset using the least squares method. The refractive index of the epitaxial layer was calculated employing differential evolution principles. Finally, Monte Carlo simulations were conducted for sensitivity analysis to assess the reliability of the fitting results. This paper comprehensively considers multiple characteristics of light beam propagation, providing an innovative solution for determining epitaxial layer thickness via multi-beam interferometry in subsequent practical applications.

Keywords: Drude Model, Fresnel's Equation, Monte Carlo Simulation, Differential Evolution.

1. Introduction

Traditional infrared interferometry faces significant challenges as semiconductor structures grow increasingly complex[1], such as in double-layer or multi-layer heterojunctions, where spectral signals become exceptionally intricate. These challenges stem from multiple sources: I spectral signal superposition and spurious peak interference caused by multiple reflections; II weak interference signals due to strong absorption or low reflectivity of materials at specific infrared wavelengths (e.g., blackbody materials); III diffuse reflection induced by rough surfaces; IV variations in material optical properties caused by substrate impurity diffusion (e.g., Fe); and V non-uniform light source power distribution [2].

To address these challenges, precise thickness extraction has become heavily reliant on advanced algorithms rather than traditional peak-and-valley techniques. Current frontier work primarily falls into two categories: Firstly, advanced signal processing strategies, such as the VMD-LSP algorithm proposed by Sun et al. [3], which employs Variational Modal Decomposition (VMD) to separate high-frequency thickness signals from low-frequency noise substrates, combined with Lomb-Scargle Periodogram (LSP) for precise frequency extraction. This method is further supplemented by "adaptive spectral clipping" and "high-precision thickness extraction" algorithms to handle weak signals and spurious peaks. The second category comprises strategies grounded in physical modelling and global optimisation. For instance, Yu and Ma [4] established an interference model based on the Fresnel equations, employing a hybrid differential evolution-nonlinear least squares method for global optimisation. Concurrently, they necessitated the removal of material-specific anomalies such as residual ray bands. Similarly, Mirschel et al. [5] successfully overcame challenges of low reflectance and diffuse reflection by combining near-infrared hyperspectral imaging with partial least squares regression, enabling online monitoring of hidden layer thickness. These advanced algorithms aim to overcome the limitations of traditional methods, which are susceptible to noise interference and unable to utilise full spectral information.

This paper proposes a high-precision measurement method for epitaxial layer thickness based on fundamental physics and global optimisation strategies. This approach overcomes the reliance of conventional methods on specific characteristic points, significantly enhancing the robustness and accuracy of measurement results.

2. Esrablishment of a Multi-Parameter Optimised Epitaxial Layer Model

This study need only consider the case where interference fringes arise from a single reflection and transmission at the interface between the epitaxial layer and the substrate.

According to Snell's law:

$$n_0 sin\alpha_1 = n_1 sin\beta_1 \tag{1}$$

where α denotes the angle of incidence and β denotes the angle of refraction.

Thus, calculated the cosine of the angle between the beam entering the epitaxial layer from air and the beam travelling from the substrate to the epitaxial layer.

$$cos\beta_1 = \sqrt{1 - sin\beta_1{}^2} \tag{2}$$

$$cos\beta_2 = \sqrt{1 - sin\beta_2{}^2} \tag{3}$$

where cosβ represents the complex cosine angle.

Assuming the light source illuminates the SiC epitaxial layer from air, where our n_0 is approximately equal to 1, and n_1 represents the refractive index of the epitaxial layer, this study employ the Drude model complex refractive index as an approximation in this paper.

The refractive index of the epitaxial layer constitutes a significant variable that cannot be disregarded. Its value is dependent upon parameters such as the concentration of doped carriers within the epitaxial layer and the wavelength of the infrared spectrum. Consequently, this study employ the Drude model with modifications, utilising the complex refractive index denoted by N_j to calculate the refractive index n_j.

$$N_j(v) = n_j(v) + ik_j(v) \tag{4}$$

where define j = 1 for the epitaxial layer and j = 2 for the substrate.

Imposing constraints on the refractive index：

$$\begin{cases} n_j(v) > 0 \\ k_j(v) > 0 \end{cases} \tag{5}$$

Based on the core formula of the Drude model, define the complex permittivity $\epsilon_j(v)$

$$\epsilon_j(v) = \epsilon_{j,\infty} - \frac{{\omega_{pj,rad}}^2}{\omega^2 + i\gamma_{j,rad}\omega} \tag{6}$$

where the calculation formulas for $\omega_{pj,rad}$, ω, $\gamma_{j,rad}$ are as follows:

$$\begin{cases} \omega_{pj,rad} = 2\pi C\omega_{pj} \\ \omega = 2\pi C v \\ \gamma_{j,rad} = 2\pi C\gamma_j \end{cases} \tag{7}$$

where the ω represented the number of wave, and all parameters in the Drude model are converted to angular frequency units.

This study calculate the intensity and phase of the two reflections, employing the Fresnel equations to determine the reflection coefficient and transmission coefficient. The Fresnel equations describe the laws of reflection and refraction at the interface between two media, containing formulas for the reflection coefficients of both S-polarised (TE mode) and P-polarised (TM mode) light.

The mathematical definition of s-polarisation is as follows:

$$r_{ij}^s = \frac{N_i cos\theta_i - N_i cos\theta_j}{N_i cos\theta_i + N_i cos\theta_j} \tag{8}$$

The mathematical definition of p-polarisation is as follows::

$$p_{ij}^s = \frac{N_j cos\theta_i - N_i cos\theta_j}{N_j cos\theta_i + N_i cos\theta_j} \tag{9}$$

where $N_{i/j}$ denotes the complex refractive index of the medium, while $\theta_{i/j}$ represents the complex angle of incidence and the complex angle of refraction.

Then, considering the practical context of our epitaxial layer measurements, this study classify the propagation of light beams from different media into two scenarios: from air into the epitaxial layer, and from the substrate into the epitaxial layer, satisfying the equation:

$$r_{01}^s(\tilde{v}) = \frac{n_0 \cos\alpha_1 - N_1(\tilde{v})\cos\beta_1}{n_0 \cos\alpha_1 + N_1(\tilde{v})\cos\beta_1} \tag{10}$$

$$r_{01}^p(\tilde{v}) = \frac{N_1(\tilde{v})\cos\alpha_1 - n_0\cos\beta_1}{N_1(\tilde{v})\cos\alpha_1 + n_0\cos\beta_1} \tag{11}$$

where r_{01} denotes the transition from air to the epitaxial layer.

$$r_{12}^s(\tilde{v}) = \frac{N_1(\tilde{v})\cos\alpha_2 - N_2(\tilde{v})\cos\beta_2}{N_1(\tilde{v})\cos\alpha_2 + N_2(\tilde{v})\cos\beta_2} \tag{12}$$

$$r_{12}^p(\tilde{v}) = \frac{N_2(\tilde{v})\cos\alpha_2 - N_1(\tilde{v})\cos\beta_2}{N_2(\tilde{v})\cos\alpha_2 + N_1(\tilde{v})\cos\beta_2} \tag{13}$$

where r_{12} denotes the transition from air to the epitaxial layer.

The interference phenomenon occurring after two reflections of a light beam, the path difference between the two beams:

$$\delta(v) = N_1 * \frac{2\pi}{\lambda}\Delta \tag{14}$$

$$\Delta = 2\pi h N_1 cos\beta_1 \tag{15}$$

Utilising the inverse relationship between wave number and wavelength:

$$\lambda = \frac{1}{v} \tag{16}$$

where v denotes the wave number, λ denotes the wavelength, and h denotes the epitaxial layer thickness.

By combining the equations, this study derive the specific expression for the optical path difference, thereby determining the required variable in the problem: the thickness of the external layer:

$$h = \frac{\delta(v)}{4\pi v N_1(v) h cos\beta_1} \tag{17}$$

During the interference process following two reflections of the light beam on the SiC surface, this study consider the magnitude of the light beam's intensity at different interfaces

$$R_1(\tilde{v}) = \frac{1}{2}\left(|r_{01}^s(\tilde{v})|^2 + \left|r_{01}^p(\tilde{v})\right|^2\right) \tag{18}$$

$$R_2(\tilde{v}) = \frac{1}{2}\left(|r_{12}^s(\tilde{v})|^2 + \left|r_{12}^p(\tilde{v})\right|^2\right) \tag{19}$$

This paper perform vector superposition and combine the above equations to obtain the total intensity reflectance:

$$R_{total} = R_1(v) + R_2(v) + 2\sqrt{R_1(v)R_2(v)}cos\left(re(\delta(v) + \varphi_0)\right) \tag{20}$$

where 're()' denotes the complex phase, introducing φ_0 to absorb these constant phase shifts and complex problem.

3. Results

The dataset used in the experiment was sourced from: https://www.mcm.edu.cn/html_cn/node/03c91a444e62eee81a3740fa97a461a6.html

The dataset comprises test results for the same silicon carbide wafer at incident angles of 10° and 15°, alongside corresponding results for the same silicon wafer at these angles. In this experiment, this paper focus on the scenario where only a single reflection occurs at the epitaxial layer-substrate interface within the transmitted beam. Utilising the silicon carbide epitaxial wafer dataset, to determine the epitaxial layer thickness.

This paper performed global formula fitting on the respective datasets and analysed the correlation between the thickness and refractive index of the epitaxial layer in each fitted model. The Fitting results for an incident angle of 10° and 15° is shown in Figure 1 and Figure 2.

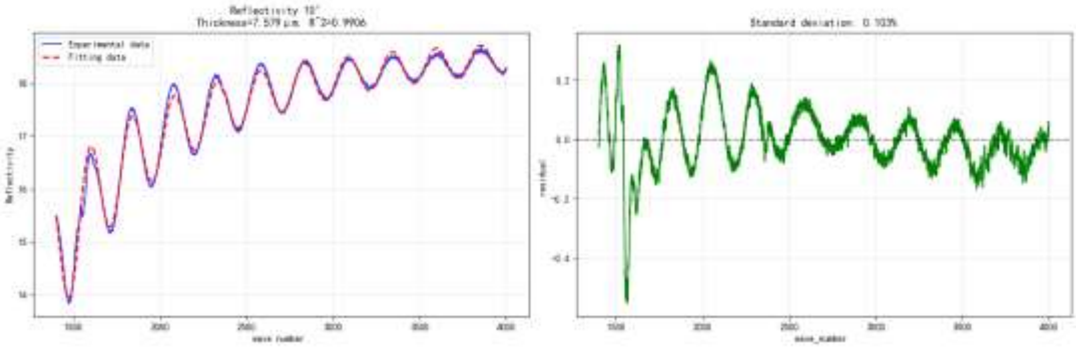

Figure 1. Fitting results for an incident angle of 10°

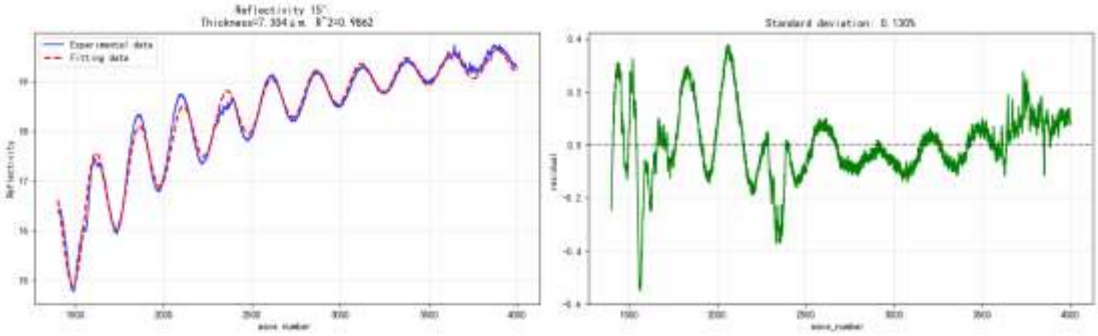

Figure 2. Fitting results for an incident angle of 15°

The data was fitted using the method of least squares, The comparison results are shown in Table 1.

Table 1. comparison results

Parameters	10° Results	15° Results	Difference(%)
Thickness	7.5789	7.3044	3.62
Epsilon1	6.4659	6.8770	6.36
Omega_p1	1679.5719	2003.1979	19.27
Gamma1	40.5704	680.4754	1577.27
Epsilon2	6.4247	6.9051	7.48
Omega_p2	1848.4823	1797.1745	2.78
Gamma2	55.2658	580.1156	949.68
Phi0	-213.1900	-193.1278	-9.41
R^2	0.9906	0.9862	/
Standard deviation	0.1032	0.1304	/

As shown in Figures 1 and Table 1, under global fitting of test results for incident angles of 10° and 15°, both exhibit excellent fitting outcomes for epitaxial layer thickness. The post-fitting R^2 values are highly satisfactory, enabling our formula to be fitted to the greatest extent possible based on known variable relationships. This indirectly validates the mathematical model established in Problem 1. Comparing the parameter variable tables for both models (Figure 3) reveals significant variation in the equation parameters requiring fitting. This stems from substantial differences in Drude model parameters across varying angles, where the required parameter values cannot be guaranteed to remain broadly similar. For instance, this may occur if the Drude model fails to fully account for all dispersion effects, or if the detection depth of the sample differs under varying incident angles.

This paper utilise the covariance matrix within the model formula to compute the standard errors and confidence intervals of the parameters, thereby conducting an uncertainty analysis, The analysis results are shown in Table 2.

Table 2. Analysis result

	Parameter uncertainty(95% CI)
Thickness	7.3044 ± 0.0023 (CI: [7.2999, 7.3089])
Epsilon1	6.8770 ± 0.0025 (CI: [6.8720, 6.8820])
Omega_p1	2003.1979 ± 6.7537 (CI: [1989.9606, 2016.4352])
Gamma1	680.4754 ± 9.1988 (CI: [662.4457, 698.5051])
Epsilon2	6.9051 ± 0.0126 (CI: [6.8804, 6.9297])
Omega_p2	1797.1745 ± 131.7490 (CI: [1538.9464, 2055.4026])
Gamma2	580.1156 ± 3550.7434 (CI: [-6379.3414, 7539.5726])
Phi0	-193.13° ± 0.92° (CI: [-194.93°, -191.33°])

At the 95% confidence interval, the fitted epitaxial layer thickness reached 7.3044 ± 0.0023. The analysis of parameter uncertainty in the figure above fully demonstrates that both our modelling approach and algorithm design have achieved significant success.

4. Conclusions

The thickness of the epitaxial layer directly determines the breakdown voltage tolerance of semiconductor devices, thereby influencing product quality issues and performance variations during operation. This paper employs a hybrid Drude-Fresnel equation model to construct a calculation framework for epitaxial layer thickness, comprehensively accounting for the particle nature of the beam itself and the physical properties of both the epitaxial layer and substrate during reflection processes. Experimental results demonstrate that this multi-parameter hybrid model exhibits excellent robustness and holds practical application value.

Under the ideal conditions described above, involving only a single reflection and refraction, a mathematical model for measuring epitaxial layer thickness was established based on physical properties. This model was subsequently validated experimentally to confirm its accuracy and reliability. Building upon this foundation, this study may in future derive a calculation method for epitaxial layer thickness under more general conditions, specifically those involving multi-beam interference. This development will significantly impact semiconductor fabrication processes.

References

[1] Ando Y, Makisako R, Takahashi H, et al. Dependence of electrical characteristics on epitaxial layer structure of AlGaN/GaN HEMTs fabricated on freestanding GaN substrates[J]. IEEE Transactions on Electron Devices, 2021, 69(1): 88-95.

[2] Park J, Cho Y J, Chegal W, et al. A review of thin-film thickness measurements using optical methods[J]. International Journal of Precision Engineering and Manufacturing, 2024, 25(8): 1725-1737.

[3] Sun J, Li Z, Zhang H, et al. An improved method for measuring epi-wafer thickness based on the infrared interference principle: Addressing interference quality and multiple interferences in double-layer structures[J]. Results in Physics, 2023, 54: 107146.

[4] Yu T, Ma T. Solving Strategy for Silicon Carbide Epitaxial Layer Thickness Based on Nonlinear Least Squares Method[J]. Frontiers in Engineering, 2025, 1(1): 45-48.

[5] Mirschel G, Daikos O, Scherzer T. In-line monitoring of the thickness distribution of adhesive layers in black textile laminates by hyperspectral imaging[J]. Computers & Chemical Engineering, 2019, 124: 317-325.